Software-Defined Event-Triggering Control for Large-Scale Networked Systems Subject to Stochastic Cyberattacks

Yan Li, Feiyu Song, Jinliang Liu, Xiangpeng Xie, and Engang Tian

***Abstract*—In large-scale networked control systems (NCSs), an important issue is how to guarantee the system performance under the limited network bandwidth and stochastic cyberattacks. Centralized event-triggering mechanisms (ETMs) are now regarded as a desirable solution to ease the bandwidth pressure, but the application in large-scale NCSs is constrained by overall management complexity. In this article, we will first propose a software-defined centralized ETM to cost-efficiently conduct an event-triggering decision based on global system states to ensure system transmission performance. Then, by taking deception attacks, which can hardly be detected and pose serious threats to NCSs into account, we study a secure control problem over a large-scale NCS with the presented centralized ETM. The considered deception attacks compromise controller-to-actuator channels, and the specific behaviors of the attacks on different channels are depicted by different Bernoulli processes. To solve the problem, a formal model of the envisioned large-scale system is established, the sufficient conditions that achieve the uniformly ultimately bounded stability of the formulated system are analyzed, and then the controller gains are designed accordingly. The effectiveness of the proposed approach is finally validated by an illustrative example.**

***Index Terms*—Centralized event-triggering mechanisms (ETMs), deception attacks, large-scale networked control systems (NCSs), software-defined networking (SDN), uniformly ultimately bounded (UUB).**

Manuscript received 22 October 2022; accepted 28 December 2022. Date of publication 4 January 2023; date of current version 17 August 2023. This work was supported in part by the National Natural Science Foundation of China under Grant 61973152, Grant 62022044 and Grant 62273174, in part by the Natural Science Foundation of Jiangsu Province of China under Grant BK20211290, in part by the Postgraduate Research and Practice Innovation Program of Jiangsu Province under Grant SFYXW21001, and in part by the Qing Lan Project. Recommended by Associate Editor K. You. *(Corresponding author: Jinliang Liu.)*

Yan Li, Feiyu Song, and Jinliang Liu are with the College of Information Engineering, Nanjing University of Finance and Economics, Nanjing 210023, China (e-mail: ylnjue@163.com; songfeiyu29@163.com; liujinliang@vip.163.com).

Xiangpeng Xie is with the Institute of Advanced Technology, Nanjing University of Posts and Telecommunications, Nanjing 210023, China (e-mail: xiexiangpeng1953@163.com).

Engang Tian is with the School of Optical-Electrical and Computer Engineering, University of Shanghai for Science and Technology, Shanghai 200093, China (e-mail: tianengang@163.com).

Digital Object Identifier 10.1109/TCNS.2022.3233925

I. Introduction

OVER the past few decades, networked control systems (NCSs) have attracted considerable attention with the development of communication technology [1], [2], [3]. Compared with traditional control systems, system components in NCSs, such as sensors, controllers, and actuators, are interconnected by wired or wireless networks rather than point-to-point links. This offers advantages in easing installation, maintenance, and adjustment, as well as improving flexibility, reliability, and scalability [4], [5], [6]. The merits enable extensive applications of NCSs in diverse areas. Meanwhile, the scale of NCSs is continuously expanding with the growing maturity of component techniques and increasing complexity of system tasks, and consequently, multiple subsystems are being placed in one NCS.

The large-scale NCSs composed of a number of subsystems have been successfully utilized to model many physical systems, e.g., urban transportation systems [7], electrical power systems [8], and digital communication systems [9], [10]. Despite the prevalence of large-scale NCSs, some challenges still exist in practical applications. One of the important issues is how to effectively utilize the limited network bandwidth so as to guarantee the system performance by designing appropriate data transmission mechanisms. To this end, event-triggering mechanisms (ETMs) are gaining extensive research attention (see, e.g., [11], [12], and [13]). By employing ETMs, the sampled data can be transferred only, while the predefined condition is satisfied, which significantly reduces the redundant data transmission.

The existing ETMs designed for large-scale NCSs can be mainly classified into two types: 1) decentralized ETMs and 2) centralized ETMs. For the first type of mechanism, whether the sampled data from each distributed sensor can be released into the communication network is independently decided based on the local state of its affiliated subsystem, so it is avoided to collect the global state of the system with considerable complexity. Up to now, abundant research on decentralized ETMs has been presented [14], [15], [16]. For instance, the dynamic output feedback control problem over large-scale systems based on the decentralized ETM was studied in [14]. In [15], an asynchronous-sampling-based decentralized ETM was proposed for switched large-scale systems with network delay and disturbance. However, in these schemes, the synchronized measurements among sensing nodes are generally required, and

an event detector needs to be deployed at each sensor, which inevitably incurs additional implementation cost. For the second type of mechanism, whether the sampled data in each subsystem can be transmitted is determined by a central event detector based on the predesigned global-state-dependent triggering condition, and then, the synchronization among sensors can be achieved naturally. Du et al. [17] proposed a centralized ETM to settle the leader-following consensus problem for multiagent systems with general dynamics. The synchronization problem for Markovian switching complex networks with noise and unknown transitional rates was exploited by applying the centralized ETM in [18]. Nevertheless, the management complexity in centralized ETMs is increasing with the expansion of system scale, which will limit the application of such mechanisms in large-scale NCSs.

As an emerging technology, software-defined networking (SDN) can just mitigate the discussed dilemma of centralized ETMs in large-scale NCSs. SDN is a networking paradigm that decouples the control plane from the data plane so as to significantly reduce the network management complexity. If the SDN-based centralized ETM is enabled, state messages generated by subsystems will be forwarded to an SDN controller via a dedicated channel; then, the controller will make a centralized decision on the delivery of the sampled data and notify each subsystem about the decision. Given that such control of the "events" generation is separated with a physical data plane, the scalability of the SDN-based centralized ETM can be ensured. Recently, considering the desirable properties of SDN, many research works have been conducted to integrate SDN with cyber-physical systems (CPSs) and then efficiently realize various functional requirements. For example, a discussion on the trends, challenges, and opportunities in software-defined CPSs was presented in [19]. To optimize the task scheduling in CPSs, SDN technology was adopted in [20] to realize an integrated control center so as to dynamically adjust the task scheduling strategy. Wang et al. [21] proposed an efficient SDN-based handover authentication scheme for mobile edge computing in CPSs to deal with the problems in security provisioning. In [22], a blockchain-empowered distributed software-defined CPS framework was designed to realize consensus and distributed resource management. However, to the best of our knowledge, none of the existing studies focus on incorporating SDN into NCSs to efficiently enable the centralized ETM, which greatly motivates the consideration of this article.

During the practical application of large-scale systems, another critical challenge is how to effectively defend against stochastic cyberattacks considering the openness of the communication network. Various attacks launched by adversaries will largely degrade system performance and even lead to system paralysis [23], [24], [25], [26]. Among these are deception attacks, which are acknowledged as a typical type of attack that seriously threatens the data integrity by injecting false data into original signals. To enhance the security of NCSs subject to deception attacks, a lot of research attention has been devoted [27], [28]. Focusing on large-scale NCSs, it is demanding to consider asynchronous deception attacks, which means that the communication network is divided into multiple channels, each of which is independently compromised by different deception attacks. Under the scenario of asynchronous deception attacks, Sun et al. [29] discussed the control problem for a class of network-based state-dependent uncertain systems. For multiagent systems with multiple channels, the sampled-based consensus issue was studied under deception attacks in [30]. The aforementioned works are all concerned with deception attacks occurring on sensor-to-controller channels, but the communication channels between controllers and actuators are also vulnerable to deception attacks. Based on the consideration of deception attacks that occur on controller-to-actuator channels, the synchronization control for multiagent systems was studied in [31], while the secure synchronization method was designed for coupled complex networks with nonlinearity in [32]. Nevertheless, the exploration to the issue of centralized event-triggering control for large-scale NCSs with asynchronous deception attacks that happened on controller-to-actuator channels is rarely presented, which is another motivation of this study.

In this article, under the scenario that the communication network is bandwidth limited and at the risk of asynchronous deception attacks, we will study how to design decentralized controllers under the SDN-based centralized ETM to enhance the transmission performance and security of large-scale NCSs. The major contributions of this article can be listed as follows.

1) A system architecture that integrates SDN with a large-scale NCS is built to support the efficient and scalable realization of a centralized ETM with three phases, i.e., state collection, execution of event-triggering algorithm (ETA), and decision notification.
2) Over the SDN-enabled large-scale NCS, by quantitatively and differentially evaluating the state fluctuation of each subsystem, a specific centralized ETA is proposed to guarantee the system performance under the limited communication bandwidth.
3) Based on the proposed ETM and taking asynchronous deception attacks into consideration, the model of the large-scale NCS is established to give a formal description to the studied problem.
4) The sufficient conditions for the stability of the formulated system are analyzed, and then a design method for the secure controllers is presented.

The rest of this article is organized as follows. Section II describes the proposed SDN-enabled large-scale NCS architecture for enabling the centralized ETM, and the basic model of the envisioned system. In Section III, a centralized ETA is first designed, which is followed by the formulation of the studied secure control problem and some preliminaries. The solution to the formulated problem is presented in Section IV. An illustrative example is provided in Section V to verify the effectiveness of this article. Finally, Section VI concludes this article.

II. System Architecture and Model

In this section, we first propose a system architecture that integrates SDN with a large-scale NCS to efficiently support

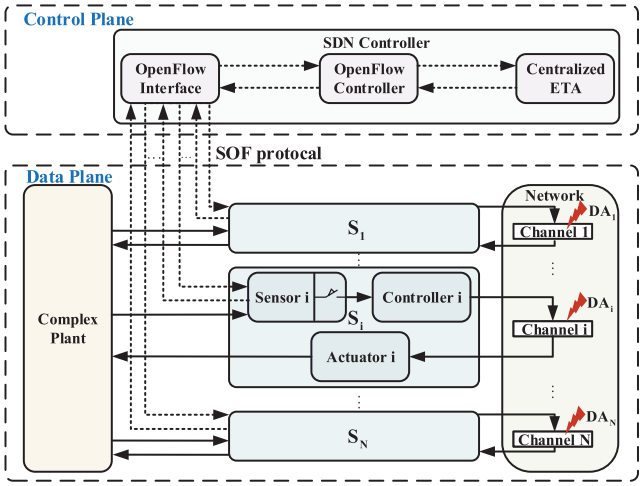

Fig. 1. SDN-enabled large-scale NCS architecture.

the centralized ETM. Then, the basic model of the considered large-scale NCS is formally introduced.

A. Architecture of the SDN-Integrated Large-Scale NCS

The proposed SDN-enabled large-scale NCS architecture is shown in Fig. 1, which is composed of two planes, i.e., data plane and control plane. The data plane consists of an NCS with N subsystems, each of which is denoted by S_i $(1 \leq i \leq N)$, and the sensor, controller, and actuator are included in each S_i. A multichannel communication network is employed to undertake the data transmission between each pair of controllers and actuators, and the network is envisioned to suffer from asynchronous deception attacks. To be specific, the channel i served for S_i will be independently compromised by a deception attack, which is referred to as DA_i. Furthermore, whether the sampled data of sensors are released into the communication network is decided by a centralized ETA conducted in the control plane, so the sensors are important components connecting the data plane and the control plane.

For the practical communication between the two planes, the standard SDN southbound protocol should be adopted. In the proposed architecture, the Sensor OpenFlow (SOF) protocol [33], which is a modification of the most popular SDN protocol, i.e., OpenFlow protocol, is employed to support the communication between the sensors and the control plane. Then, in the architecture, we have the following.

1) *For each sensor*, a compatible SOF interface (switch) is equipped to send state information of the corresponding subsystem to the SDN controller, as well as a receive decision made by the centralized ETA via SOF channel.
2) *For the SDN controller*, given that it is realized with a focus on enabling the centralized ETM, a specific OpenFlow controller, such as NOX, POX, FloodLight, and Trema [34], is deployed in the control plane. It will be responsible for collecting state information of subsystems from N sensors (such information is used to conduct the centralized ETA) and sending decision messages (such messages are generated based on the centralized ETA) to each of the sensors via OpenFlow interface.

Remark 1: Based on the SDN-integrated architecture, the envisioned centralized ETM will be implemented within three phases: the SDN controller first collects the state of each subsystem; then, the centralized ETA (which will be designed shortly) is conducted to make an event-triggering decision; and the decision is finally conveyed to all the sensors for notifying them whether the sampled data can be released into the communication network. In such a process, the communication between sensors and the SDN controller (see dotted lines) is independent of the signal transmission in the physical system (see solid lines) and, thus, the management cost introduced by the centralized ETM can be controlled validly.

Remark 2: In the designed architecture, the SDN controller is realized with the aim of cost-efficiently supporting the centralized ETM and, thus, only the data plane and the control plane are considered. Actually, the SDN controller can also undertake many other tasks, such as bandwidth allocation, system monitoring, and intrusion detection. Under a multitask scenario, an application plane can be further constructed to promote the extension of the control plane so as to provide diverse services.

B. Basic System Model

Based on the above introduced system architecture, the basic model of the considered large-scale NCS in the data plane is given as [35] and [36]

$$\dot{x}(t) = Ax(t) + Bu(t) + g(t, x(t)) + f(t, x(t), u(t)). \quad (1)$$

The system is composed of N subsystems, and each S_i $(1 \leq i \leq N)$ is formulated as

$$\dot{x}_i(t) = A_i x_i(t) + B_i u_i(t) + g_i(t, x_i(t)) \quad (2)$$

where $x_i(t) \in \mathbb{R}^{n_i}$ and $u_i(t) \in \mathbb{R}^{m_i}$ are the state vector and the control input of S_i, respectively; A_i and B_i are constant matrices of appropriate dimensions; and $g_i : \mathbb{R} \times \mathbb{R}^{n_i} \to \mathbb{R}^{n_i}$ indicates the uncertainty of the structure of S_i and is independent of other subsystems. Therefore, in (1), $x(t) = [x_1^T(t), x_2^T(t), \ldots, x_N^T(t)]^T$ and $u(t) = [u_1^T(t), u_2^T(t), \ldots, u_N^T(t)]^T$ denote the state vector and the control input of the whole system, respectively; obviously, $x(t) \in \mathbb{R}^n$ and $u(t) \in \mathbb{R}^m$, where $n = \sum_{i=1}^N n_i$ and $m = \sum_{i=1}^N m_i$; $f : \mathbb{R} \times \mathbb{R}^n \times \mathbb{R}^m \to \mathbb{R}^n$ represents the coupled interconnection function; and $A = \text{diag}\{A_1, A_2, \ldots, A_N\}$, $B = \text{diag}\{B_1, B_2, \ldots, B_N\}$, and $g(t, x(t)) = [g_1^T(t, x_1(t)), g_2^T(t, x_2(t)), \ldots, g_N^T(t, x_N(t))]^T$.

Assumption 1 (See [36]): We suppose that the structured uncertainty $g_i(t, x_i(t))$ satisfies

$$\| g_i(t, x_i(t)) \|^2 \leq \| G_i x_i(t) \|^2 \quad \forall (t, x_i(t)) \in \mathbb{R} \times \mathbb{R}^{n_i} \quad (3)$$

where $G_i \in \mathbb{R}^{n_i \times n_i}$. Then, for the decoupled nonlinear function $g(t, x(t))$, we obtain

$$\| g(t, x(t)) \|^2 \leq \| Gx(t) \|^2 \quad \forall (t, x(t)) \in \mathbb{R} \times \mathbb{R}^n \quad (4)$$

where $G = \text{diag}\{G_1, G_2, \ldots, G_N\}$.

Assumption 2 (See [37]): For the coupled nonlinear function $f(t, x(t), u(t))$, we assume that

$$\| f(t, x(t), u(t)) \|^2 \leq \| F_1 x(t) \|^2 + \| F_2 u(t) \|^2 \quad (5)$$

where $F_1 \in \mathbb{R}^{n\times n}$ and $F_2 \in \mathbb{R}^{m\times m}$.

III. Problem Formulation

Over the considered SDN-integrated large-scale NCS, the centralized ETM can be supported in a cost-efficient manner, so we first dedicate to propose a novel centralized ETA in this section. Then, by further taking asynchronous deception attacks into consideration, the formulation of the studied secure control problem is presented.

A. Dynamic Weighted Centralized ETA (DWC-ETA)

In centralized ETMs, the full states of the system will be collected and centrally measured. Then, a typical centralized ETA can be described as follows [38]:

$$\|x(t_k h + jh) - x(t_k h)\| \geq \Gamma \quad (6)$$

where h is a constant sampling period; $t_k h$ denotes the latest triggering instant, while $t_k h + jh$ represents the current sampling instant; $x(t_k h)$ and $x(t_k h + jh)$ indicate the latest transmitted data and the current sampling data, respectively; and $\Gamma > 0$ is a given threshold. In the algorithm, the norm of the state fluctuation of the whole system is calculated; then, an "event" is generated if the value exceeds Γ. However, the contributions of each subsystem for the event-triggering decision cannot be explicitly differentiated. Actually, it is desirable to give higher weights for the subsystems with a larger state fluctuation in (6) to accelerate the system transient process.

Inspired by this and considering $\|x(t_k h + jh) - x(t_k h)\|^2 = \sum_{i=1}^{N} \|x_i(t_k h + jh) - x_i(t_k h)\|^2$, we then propose a DWC-ETA based on (6), i.e.,

$$\sum_{i=1}^{N} \alpha_i(t) \|x_i(t_k h + jh) - x_i(t_k h)\|^2 \geq \gamma \quad (7)$$

where $\gamma = \frac{\Gamma^2}{N}$ is the predesigned threshold while $\alpha_i(t)$ $(1 \leq i \leq N)$ is the normalized weight assigned for S_i, and it will vary with the change of the state of S_i, specifically, $\alpha_i(t) = \frac{\delta_i(t)}{\sum_{i=1}^{N} \delta_i(t)}$ and $\delta_i(t)$ is defined as

$$\delta_i(t) = \delta_i^l + \delta_i^u e^{-\eta_i \|x_i(t_k h + jh) - x_i(t_k h)\|^{-1}} \quad (8)$$

in which δ_i^l, δ_i^u, and η_i are the given positive parameters. Apparently, $\delta_i^l \leq \delta_i(t) \leq \delta_i^l + \delta_i^u \triangleq \delta_i$ and, thus, $\frac{\delta_i^l}{\sum_{i=1}^{N} \delta_i} \triangleq \alpha_i \leq \alpha_i(t) \leq 1$.

Remark 3: In (8), $\delta_i(t)$ is a state-dependent function, i.e., the value of $\delta_i(t)$ is calculated based on the norm of the state difference between the current sampled data $x_i(t_k h + jh)$ and the latest transmitted data $x_i(t_k h)$. The greater the quantitative value of the difference, the larger the value of $\delta_i(t)$. The parameter δ_i^u can be adjusted to vary the proportion of $\|x_i(t_k h + jh) - x_i(t_k h)\|$ in (8), while η_i denotes the gradient of the exponential function.

Remark 4: For the proposed DWC-ETA, if $\alpha_i(t)$ is set to be $\frac{1}{N}$, then (7) is reduced to $\|x(t_k h + jh) - x(t_k h)\|^2 \geq \Gamma^2$, which is equivalent to the centralized ETA described in (6). Otherwise, if $\alpha_i(t) \in [0, 1]$, the sampled data in each S_i can be transmitted only, while the condition depicted by (7) is satisfied.

On the basis of the introduced DWC-ETA, the next triggering instant $t_{k+1} h$ can be written as

$$t_{k+1} h = t_k h + \min \left\{ jh | \sum_{i=1}^{N} \alpha_i(t) \|x_i(t_k h + jh) - x_i(t_k h)\|^2 \geq \gamma \right\}. \quad (9)$$

Then, the control input of S_i $(1 \leq i \leq N)$ can be described as follows:

$$u_i(t) = K_i x_i(t_k h), \quad t \in [t_k h, t_{k+1} h) \quad (10)$$

where K_i is the controller gain matrix.

For convenience of analysis, the time interval $\Pi(t_k) = [t_k h, t_{k+1} h)$ is divided into $l_M(t_k)$ subintervals as follows:

$$\begin{cases} \Lambda_0(t_k) = [t_k h, t_k h + h) \\ \vdots \\ \Lambda_l(t_k) = [t_k h + lh, t_k h + lh + h) \\ \vdots \\ \Lambda_{l_M(t_k)}(t_k) = [t_k h + l_M(t_k) h, t_{k+1} h) \end{cases} \quad (11)$$

where $l_M(t_k) = t_{k+1} - t_k - 1$ and $l = 1, 2, \ldots, l_M(t_k) - 1$. Thus, we have $\Pi(t_k) = \cup_{d=0}^{l_M(t_k)} \Lambda_d(t_k)$. We then define two piecewise functions

$$\tau(t) = \begin{cases} t - t_k h, & t \in \Lambda_0(t_k) \\ t - t_k h - h, & t \in \Lambda_1(t_k) \\ \vdots \\ t - t_k h - l_M(t_k) h, & t \in \Lambda_{l_M(t_k)}(t_k) \end{cases} \quad (12)$$

$$e_i(t) = \begin{cases} 0, & t \in \Lambda_0(t_k) \\ x_i(t_k h) - x_i(t_k h + h), & t \in \Lambda_1(t_k) \\ \vdots \\ x_i(t_k h) - x_i(t_k h + l_M(t_k) h), & t \in \Lambda_{l_M(t_k)}(t_k). \end{cases} \quad (13)$$

Obviously, $0 \leq \tau(t) < h$.

According to the above two functions, $x_i(t_k h)$ can be described as

$$x_i(t_k h) = x_i(t - \tau(t)) + e_i(t), \quad t \in \Pi(t_k). \quad (14)$$

Then, the DWC-ETA described by (7) can be rewritten as

$$\sum_{i=1}^{N} \alpha_i(t) (\|e_i(t)\|^2) \geq \gamma. \quad (15)$$

Combining (10) and (14), the control input of S_i $(1 \leq i \leq N)$ can be reexpressed as

$$u_i(t) = K_i [x_i(t - \tau(t)) + e_i(t)], \quad t \in \Pi(t_k). \quad (16)$$

Remark 5: Although the centralized ETM is proposed to efficiently reduce network load based on the constructed SDN-integrated architecture, the control method designed for the system is decentralized, i.e., a dedicated controller is equipped in each S_i $(1 \leq i \leq N)$, as shown in Fig. 1. The reason is that the high computation complexity of the centralized controller design for large-scale NCSs can hardly be decreased even under the SDN paradigm. Such a centralized-ETM-based decentralized control pattern for NCSs has been presented in existing research, e.g., [39] and [40], which validates the feasibility of our work.

B. Formulation of the Considered Secure Control Problem

Given that the controller-to-actuator communication channels are assumed to be compromised by asynchronous deception attacks, the actual signals arrived at actuators cannot be directly depicted by (16). Thus, we then take deception attacks into account to formulate the secure control problem over the large-scale NCS with the proposed DWC-ETM.

Under stochastic deception attacks, the control input of S_i $(1 \leq i \leq N)$ can be represented as

$$\hat{u}_i(t) = \beta_i(t)h_i(u_i(t)) + (1-\beta_i(t))u_i(t) \tag{17}$$

in which $h_i(u_i(t))$ indicates the energy-bounded deception signal, $\beta_i(t) \in \{0,1\}$ is a Bernoulli variable with $\text{Prob}\{\beta_i(t) = 1\} = \bar{\beta}_i$ (i.e., $\text{Prob}\{\beta_i(t) = 0\} = 1 - \bar{\beta}_i$), and $\beta_i(t) = 1$ denotes that S_i is attacked by DA_i and vice versa.

Assumption 3: The function of the randomly occurring DA_i $(1 \leq i \leq N)$, i.e., $h_i(x(\cdot))$, is assumed to satisfy

$$\|h_i(x(\cdot))\| \leq \|H_i x(\cdot)\| \tag{18}$$

where H_i is a known constant matrix representing the upper bound of the nonlinearity.

Based on (16) and (17), the basic system model described in (1) can be augmented as

$$\begin{aligned}\dot{x}(t) = {} & Ax(t) + \beta(t)Bh(u(t)) + (1-\beta(t))BK[x(t-\tau(t)) \\ & + e(t)] + g + f, \quad t \in \Pi(t_k)\end{aligned} \tag{19}$$

where $h(u(t)) = [h_1^T(u_1(t)), h_2^T(u_2(t)), \ldots, h_N^T(u_N(t))]^T$, $\beta(t) = \text{diag}\{\beta_1(t), \beta_2(t), \ldots, \beta_N(t)\}$, $x_i(t-\tau(t)) = [x_1^T(t-\tau(t)), x_2^T(t-\tau(t)), \ldots, x_N^T(t-\tau(t))]^T$, $e(t) = [e_1^T(t), e_2^T(t), \ldots, e_N^T(t)]^T$, $K = \text{diag}\{K_1, K_2, \ldots, K_N\}$, and g and f are, respectively, used to represent $g(t, x(t))$ and $f(t, x(t), \hat{u}(t))$ for brief description. Then, the studied problem is to design appropriate controllers so as to guarantee the stability of the system formulated in (19).

Remark 6: In the existing research, deception attacks considered over NCSs are mainly categorized into two types according to their occurred positions, i.e., the deception attacks occurred on the sensor-to-controller network and the deception attacks occurred on the controller-to-actuator network. For the former, the system state signal will be maliciously modified, and then, the control signal will be changed accordingly. For the latter, the control signal will be directly tampered, which is, thus, more general than the first type while studying the secure control issue over NCSs. Therefore, we take the second type of deception attacks into account in this article. Certainly, a more general/complicated scenario is that both types of deception attacks are considered simultaneously, which motivates our future work on the security control for large-scale NCSs under the complicated scenario.

Remark 7: Given that the probability of deception attacks can be obtained by monitoring attack target, we use Bernoulli variables to depict the occurrence of the considered deception attacks. Furthermore, norm-bounded functions $h_i(.)$ are adopted to model deception signals since the energy-bounded signals can enhance the concealment of attacks. The effectiveness of the presented model for deception attacks has been illustrated in many studies [28], [41].

At the end of the section, we would like to give the following definition and lemma to derive the main results.

Definition 1 (See [42]): For any initial value of $x(t)$, the formulated system (19) is said to be uniformly ultimately bounded (UUB) if there exist positive constants ϵ and $T(x(t), \epsilon)$ such that $\|x(t)\| < \epsilon$ for $\forall t > T(x(t), \epsilon)$.

Lemma 1 (See [43]): Given a time-varying function $\tau(t)$ $(t \in [0, h))$, for any constant matrices $R \in \mathbb{R}^{n\times n}$ and $U \in \mathbb{R}^{n\times n}$ satisfying $\begin{bmatrix} R & * \\ U & R \end{bmatrix} \geq 0$, the following inequality holds:

$$\begin{aligned} & -h\int_{t-h}^{t} \dot{x}^T(s)R\dot{x}(s)ds \\ & \leq \chi^T(t)\begin{bmatrix} -R & * & * \\ R-U^T & -2R+U+U^T & * \\ U^T & R-U^T & -R \end{bmatrix}\chi(t) \end{aligned} \tag{20}$$

where $\chi(t) = \left[x^T(t), x^T(t-\tau(t)), x^T(t-h)\right]^T$.

IV. Main Results

In this section, the sufficient conditions to guarantee the UUB for the system described by (19) are illustrated in Theorem 1 by employing Lyapunov stability theory. Then, the secure controllers are designed based on the linear matrix inequality (LMI) technique in Theorem 2.

Theorem 1: For given positive scalars α_i, $\bar{\beta}_i$ $(1 \leq i \leq N)$, γ, ε_1, ε_2, sampling period h, and feedback gain matrix K, the system formulated as (19) is UUB if there exist symmetric positive-definite matrices P, Q, R, and U, then the following nonlinear matrix inequalities (21) and (22) can be obtained:

$$\Phi = \begin{bmatrix} \Xi_1 & * & * & * & * & * & * \\ \Xi_2 & \Xi_8 & * & * & * & * & * \\ \Xi_3 & 0 & \Xi_8 & * & * & * & * \\ \Xi_4 & 0 & 0 & -I & * & * & * \\ \Xi_5 & 0 & 0 & 0 & -\varepsilon_2 I & * & * \\ \Xi_6 & 0 & 0 & 0 & 0 & -\varepsilon_2 I & * \\ \Xi_7 & 0 & 0 & 0 & 0 & 0 & \Xi_9 \end{bmatrix} < 0 \tag{21}$$

$$\begin{bmatrix} R & * \\ U & R \end{bmatrix} \geq 0 \tag{22}$$

where $\Xi_1 = \begin{bmatrix}\Xi_{11} & \Xi_{12}\end{bmatrix}, \Xi_2 = \begin{bmatrix}\Xi_{21} & \Xi_{22}\end{bmatrix}$

$$\Xi_{11} = \begin{bmatrix} \Delta_1 & \Delta_2^T & U^T \\ \Delta_2 & \Delta_3 & R^T - U^T \\ U & R-U & -Q-R \\ (I-\bar{\beta})K^TB^TP & 0 & 0 \\ \hat{\beta}B^TP & 0 & 0 \\ P & 0 & 0 \\ P & 0 & 0 \end{bmatrix}$$

$$\Xi_{12} = \begin{bmatrix} (I-\bar{\beta})PBK & \hat{\beta}PB & P^T & P^T \\ 0 & 0 & 0 & 0 \\ 0 & 0 & 0 & 0 \\ -\tilde{a} & 0 & 0 & 0 \\ 0 & -I & 0 & 0 \\ 0 & 0 & -\varepsilon_1^{-1}I & 0 \\ 0 & 0 & 0 & -\varepsilon_2^{-1}I \end{bmatrix}$$

$$\Delta_1 = PA + A^TP + Q + \sqrt{\gamma}I - R$$

$$\Delta_2 = (I-\bar{\beta})K^TB^TP + R - U, \Delta_3 = -2R + U + U^T$$

$$\tilde{\alpha} = \text{diag}\{\alpha_1 I_{n_1\times n_1}, \alpha_2 I_{n_2\times n_2}, \ldots \alpha_N I_{n_N\times n_N}\}$$

$$\tilde{\beta} = \text{diag}\left\{\sqrt{\bar{\beta}_1(1-\bar{\beta}_1)}, \sqrt{\bar{\beta}_2(1-\bar{\beta}_2)}, \ldots, \sqrt{\bar{\beta}_N(1-\bar{\beta}_N)}\right\}$$

$$\Xi_{21} = \begin{bmatrix} hPA & h(I-\bar{\beta})PBK & 0 & h(I-\bar{\beta})PBK \end{bmatrix}$$

$$\Xi_{22} = \begin{bmatrix} h\bar{\beta}PB & hP & hP \end{bmatrix}, H = \text{diag}\{H_1, H_2, \ldots, H_N\}$$

$$\Xi_3 = \begin{bmatrix} 0 & -h\tilde{\beta}PBK & 0 & -h\tilde{\beta}PBK & h\tilde{\beta}PB & 0 & 0 \end{bmatrix}$$

$$\Xi_4 = \begin{bmatrix} 0 & HK & 0 & HK & 0 & 0 & 0 \end{bmatrix}$$

$$\Xi_5 = \begin{bmatrix} 0 & (I-\bar{\beta})F_2K & 0 & (I-\bar{\beta})F_2K & \bar{\beta}F_2 & 0 & 0 \end{bmatrix}$$

$$\Xi_6 = \begin{bmatrix} 0 & -\tilde{\beta}F_2K & 0 & -\tilde{\beta}F_2K & \tilde{\beta}F_2 & 0 & 0 \end{bmatrix}$$

$$\Xi_7 = \begin{bmatrix} G & 0 & 0 & 0 & 0 & 0 & 0 \\ F_1 & 0 & 0 & 0 & 0 & 0 & 0 \end{bmatrix}, \Xi_8 = -PR^{-1}P$$

$$\Xi_9 = \begin{bmatrix} -\varepsilon_1 I & 0 \\ 0 & -\varepsilon_2 I \end{bmatrix}. \bar{\beta} = \text{diag}\{\bar{\beta}_1, \bar{\beta}_2, \ldots, \bar{\beta}_N\}.$$

Proof: In terms of the system (19), we construct a Lyapunov function as follows:

$$V(t) = V_1(t) + V_2(t) + V_3(t) \tag{23}$$

where

$$V_1(t) = x^T(t)Px(t)$$

$$V_2(t) = \int_{t-h}^{t} x^T(s)Qx(s)ds$$

$$V_3(t) = h\int_{-h}^{0}\int_{t+\theta}^{t} \dot{x}^T(s)R\dot{x}(s)dsd\theta.$$

Then, taking derivative and expectation on $V_w(t)$ $(w = 1, 2, 3)$, we have

$$E\{\mathcal{L}V_1(t)\} = 2x^T(t)PE\{\dot{x}(t)\} \tag{24}$$

$$E\{\mathcal{L}V_2(t)\} = x^T(t)Qx(t) - x^T(t-h)Qx(t-h) \tag{25}$$

$$E\{\mathcal{L}V_3(t)\} = h^2E\{\dot{x}^T(t)R\dot{x}(t)\} - h\int_{t-h}^{t}\dot{x}^T(s)R\dot{x}(s)ds. \tag{26}$$

We notice that $E\{\beta(t)\} = \bar{\beta}$, $E\{(\beta(t)-\bar{\beta})^2\} = \tilde{\beta}^2$, so the following equations can be obtained:

$$E\left\{\dot{x}^T(t)R\dot{x}(t)\right\} = \mathcal{A}^TR\mathcal{A} + \tilde{\beta}^2\mathcal{B}^TR\mathcal{B} \tag{27}$$

$$E\left\{\hat{u}^T(t)F_2^TF_2\hat{u}(t)\right\} = \mathcal{C}^TF_2^TF_2\mathcal{C} + \tilde{\beta}^2\mathcal{D}^TF_2^TF_2\mathcal{D} \tag{28}$$

where $\mathcal{A} = Ax(t) + \bar{\beta}Bh(u(t)) + (I-\bar{\beta})BK[x(t-\tau(t)) + e(t)] + g + f$, $\mathcal{B} = Bh(u(t)) - BK[x(t-\tau(t)) + e(t)]$, $\mathcal{C} = \bar{\beta}h(u(t)) + (1-\bar{\beta})K[x(t-\tau(t)) + e(t)]$, and $\mathcal{D} = h(u(t)) - K[x(t-\tau(t)) + e(t)]$.

By employing Lemma 1, for any appropriately dimensioned matrices R and U satisfying (22), it can be derived that

$$-h\int_{t-h}^{t}\dot{x}^T(s)R\dot{x}(s)ds \le \chi^T(t)L\chi(t) \tag{29}$$

where

$$\chi(t) = \begin{bmatrix} x(t) \\ x(t-\tau(t)) \\ x(t-h) \end{bmatrix}, L = \begin{bmatrix} -R & * & * \\ R-U^T & W & * \\ U^T & R-U^T & -R \end{bmatrix},$$

$W = -2R + U + U^T$.

Based on Assumptions 1 and 2, for $\varepsilon_1 > 0$, we obtain

$$\varepsilon_1^{-1}\|g(t, x(t))\|^2 \le \varepsilon_1^{-1}\|Gx(t)\|^2 \tag{30}$$

and for $\varepsilon_2 > 0$, we obtain

$$\varepsilon_2^{-1}\|f(t, x(t), u(t))\|^2 \le \varepsilon_2^{-1}\|F_1x(t)\|^2 + \varepsilon_2^{-1}\|F_2u(t)\|^2. \tag{31}$$

Meanwhile, according to Assumption 3, we obtain

$$h^T(u(t))h(u(t)) \le u^T(t)H^THu(t). \tag{32}$$

Thus, by combining (24)–(32), we have

$$\begin{aligned}\mathbb{E}\{\mathcal{L}V(t)\} \le\ & 2x^T(t)P\{Ax(t) + \bar{\beta}Bh(u(t)) + g + f \\ & + (I-\bar{\beta})BK[x(t-\tau(t)) + e(t)]\} + x^T(t)Qx(t) \\ & - x^T(t-h)Qx(t-h) + h^2(\mathcal{A}^TR\mathcal{A} \\ & + \tilde{\beta}^2\mathcal{B}^TR\mathcal{B}) + \chi^T(t)L\chi(t) - h^T(u(t))h(u(t)) \\ & + \{K[x(t-\tau(t)) + e(t)]\}^TH^TH\{K[x(t-\tau(t)) \\ & + e(t)]\} + \varepsilon_1^{-1}x^T(t)G^TGx(t) - \varepsilon_1^{-1}g^Tg \\ & - \varepsilon_2^{-1}f^Tf + \varepsilon_2^{-1}x^T(t)F_1^TF_1x(t) \\ & + \varepsilon_2^{-1}\mathcal{C}^TF_2^TF_2\mathcal{C} + \varepsilon_2^{-1}\tilde{\beta}^2\mathcal{D}^TF_2^TF_2\mathcal{D}\end{aligned}$$

$$- \tilde{\alpha} e^T(t)e(t) + \gamma + \sqrt{\gamma} x^T(t)x(t) - \sqrt{\gamma} x^T(t)x(t). \tag{33}$$

Then, based on Schur complement equivalence, it is clear that

$$\mathbb{E}\{\mathcal{L}V(t)\} \le \xi^T(t)T\xi(t) + \gamma - \sqrt{\gamma} x^T(t)x(t) \tag{34}$$

where $T = \Xi_1 + \Xi_2^T P^{-1} R P^{-1} \Xi_2 + \Xi_3^T P^{-1} R P^{-1} \Xi_3 + \Xi_4^T I \Xi_4 + \Xi_5^T \varepsilon_2^{-1} I \Xi_5 + \Xi_6^T \varepsilon_2^{-1} I \Xi_6 + \Xi_7^T \Xi_8^{-1} \Xi_7$.

Therefore, it can be concluded that $\mathbb{E}\{\mathcal{L}V(t)\} < 0$ can be ensured by (21) and (22) if $x^T(t)x(t) > \sqrt{\gamma}$. In other words, for $t \in [t_k h, t_{k+1} h)$, $V(t)$ is decreasing when $x^T(t)x(t) > \sqrt{\gamma}$, which means that there exists an instant t_m such that for $t > t_m$, $x^T(t)x(t)$ converges to the stability bound and remains at the stability bound. Therefore, the system formulated in (19) is UUB according to Definition 1; this completes the proof. ■

Theorem 1 demonstrates the sufficient conditions assuring the UUB of the considered large-scale NCS with the assumption that the controller parameters are known in advance. To solve the secure controller design problem, we then show how to get the feedback controller gain matrix K in Theorem 2.

Theorem 2: For given positive scalars α_i, $\bar{\beta}_i$ $(1 \le i \le N)$, γ, ε_1, ε_2, κ_j $(j = 1, 2, 3, 4)$ and sampling period h, the system depicted by (19) is UUB with feedback gain $K = YX^{-1}$ if there exist symmetric positive-definite matrices X, Y, $\widetilde{Q}$, $\widetilde{R}$, and $\widetilde{U}$, such that the following LMIs hold:

$$\Phi = \begin{bmatrix} \widetilde{\Xi_1} & * & * & * & * & * & * & * \\ \widetilde{\Xi_2} & \Theta_1 & * & * & * & * & * & * \\ \widetilde{\Xi_3} & 0 & \Theta_1 & * & * & * & * & * \\ \widetilde{\Xi_4} & 0 & 0 & -I & * & * & * & * \\ \widetilde{\Xi_5} & 0 & 0 & 0 & -\varepsilon_2 I & * & * & * \\ \widetilde{\Xi_6} & 0 & 0 & 0 & 0 & -\varepsilon_2 I & * & * \\ \widetilde{\Xi_7} & 0 & 0 & 0 & 0 & 0 & \Xi_8 & * \\ \gamma^{0.25} X & 0 & 0 & 0 & 0 & 0 & 0 & -I \end{bmatrix} < 0 \tag{35}$$

$$\begin{bmatrix} \widetilde{R} & * \\ \widetilde{U} & \widetilde{R} \end{bmatrix} \ge 0 \tag{36}$$

where

$$\widetilde{\Xi_1} = \begin{bmatrix} \widetilde{\Delta_1} & * & * & * & * & * & * \\ \widetilde{\Delta_2} & \widetilde{\Delta_3} & * & * & * & * & * \\ \widetilde{U}^T & \widetilde{R} - \widetilde{U}^T & -\widetilde{Q} - \widetilde{R} & * & * & * & * \\ \widetilde{\Delta_4} & 0 & 0 & \Theta_2 & * & * & * \\ \bar{\beta} B^T & 0 & 0 & 0 & -I & * & * \\ X & 0 & 0 & 0 & 0 & \Theta_3 & * \\ X & 0 & 0 & 0 & 0 & 0 & \Theta_4 \end{bmatrix}$$

$$\widetilde{\Delta_1} = AX + XA^T + \widetilde{Q} - \widetilde{R}, \widetilde{\Delta_2} = (I - \bar{\beta}) Y^T B^T + \widetilde{R} - \widetilde{U}^T$$

$$\widetilde{\Delta_3} = -2\widetilde{R} + \widetilde{U} + \widetilde{U}^T, \widetilde{\Delta_4} = (I - \bar{\beta}) Y^T B^T$$

$$\Theta_1 = -2\kappa_1 X + \kappa_1 \kappa_1 \widetilde{R}, \Theta_2 = -2\kappa_2 X + \kappa_2 \kappa_2 \tilde{a}$$

$$\Theta_3 = -2\kappa_3 X + \kappa_3 \kappa_3 \varepsilon_1^{-1} I, \Theta_4 = -2\kappa_4 X + \kappa_4 \kappa_4 \varepsilon_2^{-1} I$$

$$\widetilde{\Xi_2} = \begin{bmatrix} hAX & h(I - \bar{\beta})BY & 0 & h\widetilde{\Delta_4}^T & h\bar{\beta}B & hX & hX \end{bmatrix}$$

$$\widetilde{\Xi_3} = \begin{bmatrix} 0 & -h\tilde{\beta}BY & 0 & -h\tilde{\beta}BY & h\tilde{\beta}B & 0 & 0 \end{bmatrix}$$

$$\widetilde{\Xi_4} = \begin{bmatrix} 0 & HY & 0 & HY & 0 & 0 & 0 \end{bmatrix}$$

$$\widetilde{\Xi_5} = \begin{bmatrix} 0 & (I - \bar{\beta})F_2 Y & 0 & (I - \bar{\beta})F_2 Y & \bar{\beta}F_2 & 0 & 0 \end{bmatrix}$$

$$\widetilde{\Xi_6} = \begin{bmatrix} 0 & -\tilde{\beta}F_2 Y & 0 & -\tilde{\beta}F_2 Y & \tilde{\beta}F_2 & 0 & 0 \end{bmatrix}$$

$$\widetilde{\Xi_7} = \begin{bmatrix} GX & 0 & 0 & 0 & 0 & 0 & 0 \\ F_1 X & 0 & 0 & 0 & 0 & 0 & 0 \end{bmatrix}.$$

Proof: According to the Schur complement method, the matrix inequality (21) holds only if the following matrix inequality holds:

$$\widehat{\Phi} = \begin{bmatrix} \widehat{\Xi_1} & * & * & * & * & * & * & * \\ \Xi_2 & \Xi_8 & * & * & * & * & * & * \\ \Xi_3 & 0 & \Xi_8 & * & * & * & * & * \\ \Xi_4 & 0 & 0 & -I & * & * & * & * \\ \Xi_5 & 0 & 0 & 0 & -\varepsilon_2 I & * & * & * \\ \Xi_6 & 0 & 0 & 0 & 0 & -\varepsilon_2 I & * & * \\ \Xi_7 & 0 & 0 & 0 & 0 & 0 & \Xi_9 & * \\ \gamma^{0.25} I & 0 & 0 & 0 & 0 & 0 & 0 & -I \end{bmatrix} < 0 \tag{37}$$

where $\widehat{\Xi_1} = \begin{bmatrix} \widehat{\Xi_{11}} & \Xi_{12} \end{bmatrix}$

$$\widehat{\Xi_{11}} = \begin{bmatrix} \widehat{\Delta_1} & \Delta_2^T & U^T \\ \Delta_2 & \Delta_3 & R^T - U^T \\ U & R - U & -Q - R \\ (I - \bar{\beta}) K^T B^T P & 0 & 0 \\ \hat{\beta} B^T P & 0 & 0 \\ P & 0 & 0 \\ P & 0 & 0 \end{bmatrix}$$

$$\Xi_{12} = \begin{bmatrix} (I - \bar{\beta}) PBK & \hat{\beta} PB & P^T & P^T \\ 0 & 0 & 0 & 0 \\ 0 & 0 & 0 & 0 \\ -\tilde{a} & 0 & 0 & 0 \\ 0 & -I & 0 & 0 \\ 0 & 0 & -\varepsilon_1^{-1} I & 0 \\ 0 & 0 & 0 & -\varepsilon_2^{-1} I \end{bmatrix}$$

$$\widehat{\Delta_1} = PA + A^T P + Q - R. \tag{38}$$

For any positive-definite matrices P, R and scalar $\kappa_1 > 0$, we obtain

$$(R - \kappa_1^{-1} P) R^{-1} (R - \kappa_1^{-1} P) \ge 0. \tag{39}$$

Then, we can derive

$$-PR^{-1}P \le -2\kappa_1 P + \kappa_1 \kappa_1 R. \tag{40}$$

Thus, by substituting $-PRP$ with $-2\kappa_1 P + \kappa_1\kappa_1 R$ into (37), it can be observed that $\widehat{\Phi} < 0$ holds when the following matrix inequality is set up:

$$\widetilde{\Phi} = \begin{bmatrix} \widehat{\Xi_1} & * & * & * & * & * & * & * \\ \Xi_2 & \widehat{\Xi_8} & * & * & * & * & * & * \\ \Xi_3 & 0 & \widehat{\Xi_8} & * & * & * & * & * \\ \Xi_4 & 0 & 0 & -I & * & * & * & * \\ \Xi_5 & 0 & 0 & 0 & -\varepsilon_2 I & * & * & * \\ \Xi_6 & 0 & 0 & 0 & 0 & -\varepsilon_2 I & * & * \\ \Xi_7 & 0 & 0 & 0 & 0 & 0 & \Xi_8 & * \\ \gamma^{0.25} I & 0 & 0 & 0 & 0 & 0 & 0 & -I \end{bmatrix} < 0 \tag{41}$$

where $\widehat{\Xi_8} = -2\kappa_1 P + \kappa_1\kappa_1 R$.

By defining $X = P^{-1}$, $Y = KX$, $C_1 = \text{diag}\{X, X, X, X, I, X, X, X, X, X, I, I, I, I, I, I\}$, $C_2 = \text{diag}\{X, X\}$, $\widetilde{Q} = XQX$, $\widetilde{R} = XRX$, and $\widetilde{U} = XUX$, premultiplying and postmultiplying (41) and (22) with C_1 and C_2, respectively, (35) and (36) can thus be obtained based on the Schur complement. Therefore, the theorem can be proved. ■

V. Simulation Results

In this section, a simulation example is conducted to demonstrate the effectiveness of the proposed method. To be specific, we consider a typical nonlinear large-scale NCS in which two inverted pendulums are connected with a spring, referred to as TPCS [36], [37]. By recurring to [37], the state dynamical equations of the TPCS are formulated as

$$[o_1(\iota_1)^2/3]\ddot{\sigma}_1 = \varpi_1 + o_1\rho(l_1/2)\sin\sigma_1 + \iota_1 F\cos(\sigma_1 - \psi) \tag{42}$$

$$[o_2(\iota_2)^2/3]\ddot{\sigma}_2 = \varpi_2 + o_2\rho(l_2/2)\sin\sigma_2 - \iota_2 F\cos(\sigma_2 - \psi) \tag{43}$$

where o_i and ι_i $(i = 1, 2)$ denote the mass and length of pendulum i, respectively, σ_i is the angular displacement of pendulum i, ϖ_i is the torque input generated by the actuator for pendulum i, ρ indicates the constant of gravity, F is the spring force, and ψ names the slope of the spring to the earth. Here, we assume that the mass of each pendulum, i.e., o_i, is uniformly distributed. Moreover, some parameters of the spring are described as

$$F = \upsilon\left(\iota_s - [L^2 + (\iota_2 - \iota_1)^2]^{1/2}\right) \tag{44}$$

$$\iota_s = \sqrt{(L + \iota_2\sin\sigma_2 - \iota_1\sin\sigma_1)^2 + (\iota_2\cos\sigma_2 - \iota_1\cos\sigma_1)^2} \tag{45}$$

$$\psi = \tan^{-1}\frac{\iota_1\cos\sigma_1 - \iota_2\cos\sigma_2}{L + \iota_2\sin\sigma_2 - \iota_1\sin\sigma_1} \tag{46}$$

in which υ is the spring constant, ι_s represents the spring length, and L denotes the distance between two pendulums. The formula of the spring length ι_s is appropriately set to guarantee that the spring force $F = 0$ under the condition $\sigma_1 = \sigma_2 = 0$. That is to say, for $\varpi_i = 0$, $(\sigma_1, \dot{\sigma_1}, \sigma_2, \dot{\sigma_2})^T = 0$ is an equilibrium of the TPCS. For the convenience of analysis, we then assume that the mass of the spring is negligible as [37].

TABLE I
Amount of Data Transmission

	DWC-ETA	TC-ETA	CD-ETA
Average number of transmitted packets per subsystem	24	20	29
Percent (%)	33.8	28.2	40.8

By defining $x(t) = [\sigma_1, \dot{\sigma_1}, \sigma_2, \dot{\sigma_2}]^T$ and $u(t) = [\varpi_1(t), \varpi_2(t)]^T$, giving parameters $o_1 = 1$ kg, $o_2 = 0.8$ kg, $\iota_1 = 1$ m, $\iota_2 = 0.8$ m, $L = 1.2$ m, $\upsilon = 0.04$ N/m, $\rho = 9.8$ m/s, and following the same analytical method presented in [36] and [37], the system model (1) under the constraints of (4) and (5) can be obtained with the following parameters:

$$A = \begin{bmatrix} -3.017 & 2.0492 & 0 & 0 \\ 0 & -2.0492 & 0 & 0 \\ 0 & 0 & -5.011 & 3.0374 \\ 0 & 0 & 0 & -3.0374 \end{bmatrix}$$

$$B = \begin{bmatrix} 1.0951 & 0 \\ 0 & 0 \\ 0 & 1.0837 \\ 0 & 0 \end{bmatrix}, g = \begin{bmatrix} 0 \\ 13.7(\sin\sigma_1 - \sigma_1) \\ 0 \\ 17.2(\sin\sigma_2 - \sigma_2) \end{bmatrix}$$

$$f = \begin{bmatrix} 0 \\ 3F(\cos(\sigma_1 - \psi)) \\ 0 \\ -4.68F(\cos(\sigma_2 - \psi)) \end{bmatrix}$$

$G = \text{diag}\{0.675, 0, 0.844, 0\}$, $F_1 = \text{diag}\{0.368, 0, 0.165, 0\}$, and $F_2 = 0$.

In the above depicted system, for each subsystem S_i $(i = 1, 2)$, the deception attack signal $h_i(u_i(t))$ is assumed to be [44]

$$h_i(u_i(t)) = 0.1u_i(t) + \tanh(0.1u_i(t)) \tag{47}$$

with the upper bound matrix $H_i = 0.2$. We further set the sampling interval $h = 0.1$ s, $\bar{\beta}_1 = 0.5$, $\bar{\beta}_2 = 0.7$, $\varepsilon_1 = \varepsilon_2 = 1$, $\gamma = 0.00001$, $\kappa_j = 1$, $(j = 1, 2, 3, 4)$, $\delta_1^l = \delta_2^l = 0.1$, $\delta_1^u = \delta_2^u = 0.9$, $\eta_1 = \eta_2 = -1$, and the state initial condition $x_1^0 = \begin{bmatrix} -2.5 & -1.5 \end{bmatrix}^T$, $x_2^0 = \begin{bmatrix} 1.3 & -0.4 \end{bmatrix}^T$.

Based on the above simulation settings, we solve LMIs presented in Theorem 2 by employing MATLAB and obtain the following feedback controller gains:

$$K_1 = \begin{bmatrix} -0.5889 & -0.3560 \end{bmatrix}, K_2 = \begin{bmatrix} -0.4446 & -0.2270 \end{bmatrix}. \tag{48}$$

Then, the simulation results are specifically presented in Figs. 2–6 and Table I.

The system state responses are shown in Fig. 2. It can be found that the stability of the simulated system is guaranteed with the proposed method. The distributions of the independent deception attacks occurred on the two subsystems are exhibited in Fig. 3. Fig. 4 describes the trajectory of the weight $\alpha_i(t)$

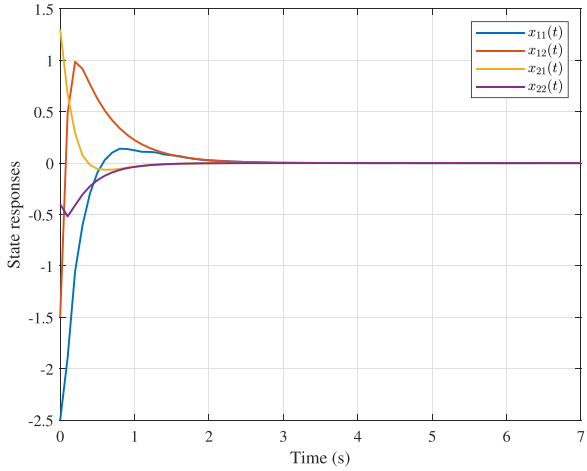

Fig. 2. State responses of x_i $(i = 1, 2)$.

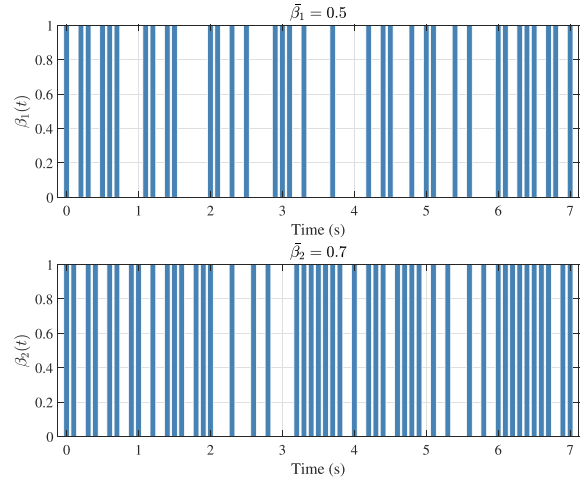

Fig. 3. Bernoulli distribution of $\beta_i(t)$ $(i = 1, 2)$.

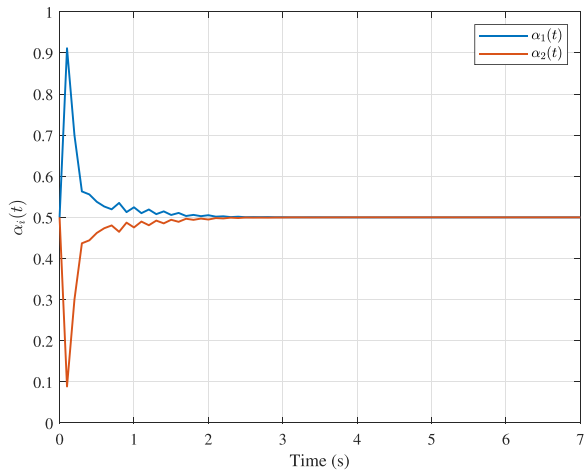

Fig. 4. Varying trajectory of $\alpha_i(t)$ $(i = 1, 2)$.

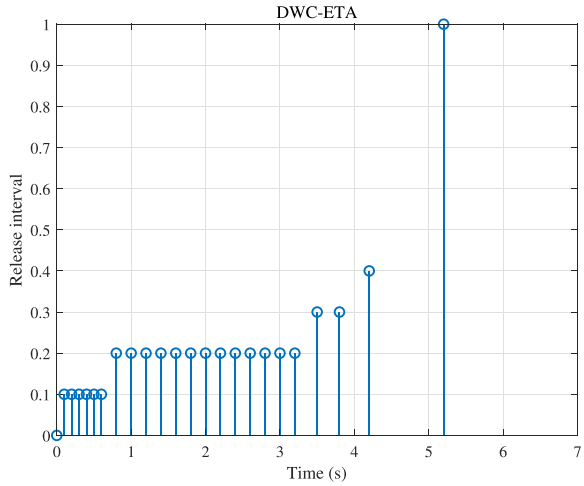

Fig. 5. Event-triggering instants and release intervals under the DWC-ETA.

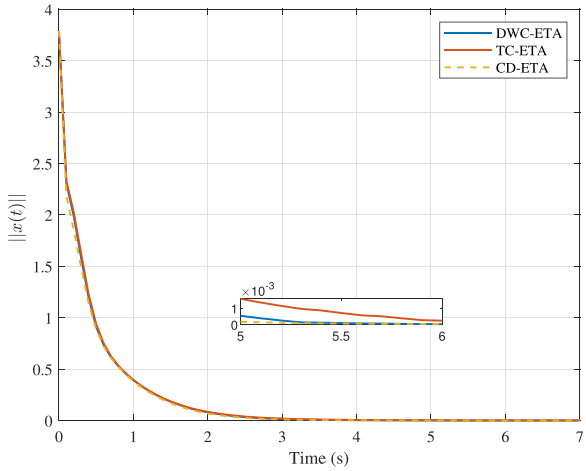

Fig. 6. $\|x(t)\|$ obtained under the three ETAs.

$(i = 1, 2)$ in the designed DWC-ETA. As shown, within 0–1 s, when the state change of S_1 is much more drastic than that of S_2 which can be seen in Fig. 2, $\alpha_1(t)$ increases from 0.5 to more than 0.9; meanwhile, $\alpha_2(t)$ decreases from 0.5 to less than 0.1. It means that the state fluctuation of S_1 plays a more important role in the DWC-ETA. The specific event-triggering instants and intervals are displayed in Fig. 5.

To illustrate the performance of the proposed DWC-ETA, we then compare it with the traditional centralized ETA (referred to as TC-ETA) presented in (6), and a classical decentralized ETA (referred to as CD-ETA) in which each subsystem independently decides the event-triggering instants according to the following condition:

$$(x_i(t_k^i h + u^i h) - x_i(t_k^i h))^T \Omega_i (x_i(t_k^i h + u^i h) - x_i(t_k^i h)) > \rho_i x_i^T(t_k^i h + u^i h) \Omega_i x_i(t_k^i h + u^i h) \quad (49)$$

where ρ_i is set to be 0.1.

As shown in Fig. 6, the transient performance of the proposed DWC-ETA is better than that of the TC-ETA since that the

time-varying weight $\alpha_i(t)$ is introduced to capture the state fluctuation of each subsystem to release performance-critical data packets (where the computation complexity of $\alpha_i(t)$ is negligible because it is calculated based on the norm of the system state fluctuation). It can also be found that the dynamic performance of the proposed DWC-ETA is very close to that of the CD-ETA where more timely response to the state change of each subsystem is enabled with the deployment of N event detectors (N is the number of subsystems); thus, the proposed DWC-ETA, which is supported by one SDN-based event detector, is a more cost-efficient ETA for reducing the system transient process.

Table I presents the amount of data transmission under each of the conducted ETAs. Generally, the improved dynamic system performance is achieved with more released data packets. Although few packets are additionally transmitted in the DWC-ETA to accelerate the stabilization of the system compared with the TC-ETA, still only 33.8% sampled data packets are released in the DWC-ETA, which already alleviates the burden of the communication network greatly.

VI. Conclusion

In this article, for the large-scale NCS subjects to limited network bandwidth and asynchronous deception attacks, we designed secure controllers to ensure the UUB stability of the system. Specifically, an SDN-based centralized ETM was proposed to alleviate the bandwidth pressure by elaborately integrating SDN into the large-scale NCS and designing an efficient DWC-ETA. The ETM can be realized without incurring high management cost and achieve good system transmission performance. Then, focusing on the asynchronous deception attacks occurred on controller-to-actuator channels, the secure control problem over the considered large-scale NCS was formulated by constructing the system model. On the basis of the established model, the sufficient conditions for the UUB of the system were presented by using Lyapunov stability theory; furthermore, the controller gains were derived via LMI technology. Finally, the efficiency of the study was demonstrated by applying the proposed method into a TPCS system.

In future work, considering that the deception attack model is constructed based on the Bernoulli process, we will extend the designed SDN-integrated architecture to cost-efficiently realize an SDN-based attack detector; then, a more realistic attack model can be established to achieve more effective secure controllers. Moreover, given that the presented SDN-based centralized ETM is only evaluated by conducting simulation based on MATLAB, we will dedicate to realize more practical emulation by using a realistic SOF-enabled SDN controller, interfaces, sensors, and implementing SOF protocol. Apparently, this work lays good foundation for the future studies.

References

[1] D. J. Antunes and H. Qu, "Frequency-domain analysis of networked control systems modeled by Markov jump linear systems," *IEEE Trans. Control Netw. Syst.*, vol. 8, no. 2, pp. 906–916, Jun. 2021.

[2] R. Kato, A. Cetinkaya, and H. Ishii, "Security analysis of linearization for nonlinear networked control systems under DoS," *IEEE Trans. Control Netw. Syst.*, vol. 8, no. 4, pp. 1692–1704, Dec. 2021.

[3] C. Ren, J. H. Park, and S. He, "Positiveness and finite-time control of dual switching Poisson jump network control systems with time-varying delays and packet drops," *IEEE Trans. Control Netw. Syst.*, vol. 9, no. 2, pp. 575–587, Jun. 2022.

[4] J. Zhang, C. Peng, X. Xie, and D. Yue, "Output feedback stabilization of networked control systems under a stochastic scheduling protocol," *IEEE Trans. Cybern.*, vol. 50, no. 6, pp. 2851–2860, Jun. 2020.

[5] L. Zha, R. Liao, J. Liu, X. Xie, E. Tian, and J. Cao, "Dynamic event-triggered output feedback control for networked systems subject to multiple cyber attacks," *IEEE Trans. Cybern.*, vol. 52, no. 12, pp. 13800–13808, Dec. 2022.

[6] A. González, Á. Cuenca, J. Salt, and J. Jacobs, "Robust stability analysis of an energy-efficient control in a networked control system with application to unmanned ground vehicles," *Inf. Sci.*, vol. 578, pp. 64–84, 2021.

[7] X. Chao, G. Kou, Y. Peng, E. Herrera-Viedma, and F. Herrera, "An efficient consensus reaching framework for large-scale social network group decision making and its application in urban resettlement," *Inf. Sci.*, vol. 575, pp. 499–527, 2021.

[8] M. Kouki, B. Marinescu, and F. Xavier, "Exhaustive modal analysis of large-scale interconnected power systems with high power electronics penetration," *IEEE Trans. Power Syst.*, vol. 35, no. 4, pp. 2759–2768, Jul. 2020.

[9] M. Ma, T. Wang, J. Qiu, and H. R. Karimi, "Adaptive fuzzy decentralized tracking control for large-scale interconnected nonlinear networked control systems," *IEEE Trans. Fuzzy Syst.*, vol. 29, no. 10, pp. 3186–3191, Oct. 2021.

[10] M. Zhao, C. Peng, Q. Han, and X. Zhang, "Cluster consensus of multiagent systems with weighted antagonistic interactions," *IEEE Trans. Cybern.*, vol. 51, no. 11, pp. 5609–5618, Nov. 2021.

[11] S. Li, X. Nian, and Z. Deng, "Distributed optimization of second-order nonlinear multiagent systems with event-triggered communication," *IEEE Trans. Control Netw. Syst.*, vol. 8, no. 4, pp. 1954–1963, Dec. 2021.

[12] J. Liu, W. Suo, X. Xie, D. Yue, and J. Cao, "Quantized control for a class of neural networks with adaptive event-triggered scheme and complex cyber-attacks," *Int. J. Robust Nonlinear Control*, vol. 31, no. 10, pp. 4705–4728, 2021.

[13] S. Gong, Z. Guo, S. Wen, and T. Huang, "Stabilization analysis for linear disturbed event-triggered control system with packet losses," *IEEE Trans. Control Netw. Syst.*, vol. 9, no. 3, pp. 1339–1347, Sep. 2022.

[14] D. Liu and G. Yang, "Decentralized event-triggered output feedback control for a class of interconnected large-scale systems," *ISA Trans.*, vol. 93, pp. 156–164, 2019.

[15] Y. Qi, N. Xing, X. Zhao, W. Guan, S. Yuan, and Z. Cao, "Asynchronous decentralized event-triggered control for switched large-scale systems subject to data congestions and disorders," *IEEE Syst. J.*, vol. 15, no. 2, pp. 2541–2552, Jun. 2021.

[16] Y. Li, F. Song, J. Liu, X. Xie, and E. Tian, "Decentralized event-triggered synchronization control for complex networks with nonperiodic DoS attacks," *Int. J. Robust Nonlinear Control*, vol. 32, no. 3, pp. 1633–1653, 2022.

[17] S. Du, T. Liu, and D. W. C. Ho, "Dynamic event-triggered control for leader-following consensus of multiagent systems," *IEEE Trans. Syst., Man, Cybern., Syst.*, vol. 50, no. 9, pp. 3243–3251, Sep. 2020.

[18] H. Dong, J. Zhou, and M. Xiao, "Centralized/decentralized event-triggered pinning synchronization of stochastic coupled networks with noise and incomplete transitional rate," *Neural Netw.*, vol. 121, pp. 10–20, 2020.

[19] E. Molina and E. Jacob, "Software-defined networking in cyber-physical systems: A survey," *Comput. Elect. Eng.*, vol. 66, pp. 407–419, 2018.

[20] X. Wang, L. Chai, Y. Zhou, and F. Dan, "Dual-network task scheduling in cyber–physical systems: A cooptimization approach," *IEEE Trans. Ind. Inform.*, vol. 17, no. 5, pp. 3143–3152, May 2021.

[21] C. Wang, Y. Zhang, X. Chen, K. Liang, and Z. Wang, "SDN-based handover authentication scheme for mobile edge computing in cyber-physical systems," *IEEE Internet Things J.*, vol. 6, no. 5, pp. 8692–8701, Oct. 2019.

[22] D. Wang, N. Zhao, B. Song, P. Lin, and F. R. Yu, "Resource management for secure computation offloading in softwarized cyber–physical systems," *IEEE Internet Things J.*, vol. 8, no. 11, pp. 9294–9304, Jun. 2021.

[23] J. Liu, T. Yin, J. Cao, D. Yue, and H. R. Karimi, "Security control for T–S fuzzy systems with adaptive event-triggered mechanism and multiple cyber-attacks," *IEEE Trans. Syst., Man, Cybern., Syst.*, vol. 51, no. 10, pp. 6544–6554, Oct. 2021.

[24] P. Griffioen, R. Romagnoli, B. H. Krogh, and B. Sinopoli, "Reducing attack vulnerabilities through decentralized event-triggered control," in *Proc. IEEE Conf. Decis. Control*, 2021, pp. 5715–5722.

[25] P. Griffioen, S. Weerakkody, and B. Sinopoli, "A moving target defense for securing cyber-physical systems," *IEEE Trans. Autom. Control*, vol. 66, no. 5, pp. 2016–2031, May 2021.

[26] C. Peng, J. Wu, and E. Tian, "Stochastic event-triggered h ∞ control for networked systems under denial of service attacks," *IEEE Trans. Syst., Man, Cybern., Syst.*, vol. 52, no. 7, pp. 4200–4210, Jul. 2022.
[27] L. Li, H. Yang, Y. Xia, and C. Zhu, "Attack detection and distributed filtering for state-saturated systems under deception attack," *IEEE Trans. Control Netw. Syst.*, vol. 8, no. 4, pp. 1918–1929, Dec. 2021.
[28] Q. Zhang, X. Yin, and S. Hu, "A two-event-generator scheme for event-triggered control of uncertain NCSs under deception attacks," *Inf. Sci.*, vol. 584, pp. 148–169, 2022.
[29] Y. Sun, J. Yu, X. Yu, and H. Gao, "Decentralized adaptive event-triggered control for a class of uncertain systems with deception attacks and its application to electronic circuits," *IEEE Trans. Circuits Syst. I: Reg. Papers*, vol. 67, no. 12, pp. 5405–5416, Dec. 2020.
[30] Y. Cui, Y. Liu, W. Zhang, and F. E. Alsaadi, "Sampled-based consensus for nonlinear multiagent systems with deception attacks: The decoupled method," *IEEE Trans. Syst., Man, Cybern., Syst.*, vol. 51, no. 1, pp. 561–573, Jan. 2021.
[31] W. He, Z. Mo, Q. Han, and F. Qian, "Secure impulsive synchronization in Lipschitz-type multi-agent systems subject to deception attacks," *IEEE/CAA J. Autom. Sinica*, vol. 7, no. 5, pp. 1326–1334, Sep. 2020.
[32] D. Ding, Z. Tang, Y. Wang, and Z. Ji, "Secure synchronization of complex networks under deception attacks against vulnerable nodes," *Appl. Math. Comput.*, vol. 399, 2021, Art. no. 126017.
[33] T. Luo, H.-P. Tan, and T. Q. S. Quek, "Sensor openflow: Enabling software-defined wireless sensor networks," *IEEE Commun. Lett.*, vol. 16, no. 11, pp. 1896–1899, Nov. 2012.
[34] A. V. Priya and N. Radhika, "Performance comparison of SDN openflow controllers," *Int. J. Comput. Aided Eng. Technol.*, vol. 11, no. 4/5, pp. 467–479, 2019.
[35] M. Ikeda and D. Šiljak, "Robust stabilization of nonlinear systems via linear state feedback," *Control Dyn. Syst.*, vol. 51, pp. 1–30, 1992.
[36] C. Peng, Q. Han, and D. Yue, "Communication-delay-distribution-dependent decentralized control for large-scale systems with IP-based communication networks," *IEEE Trans. Control Syst. Technol.*, vol. 21, no. 3, pp. 820–830, May 2013.
[37] C. Peng, E. Tian, J. Zhang, and D. Du, "Decentralized event-triggering communication scheme for large-scale systems under network environments," *Inf. Sci.*, vol. 380, pp. 132–144, 2017.
[38] J. Lunze and D. Lehmann, "A state-feedback approach to event-based control," *Automatica*, vol. 46, no. 1, pp. 211–215, 2010.
[39] C. Pasquale, S. Sacone, S. Siri, and A. Ferrara, "Hierarchical centralized/decentralized event-triggered control of multiclass traffic networks," *IEEE Trans. Control Syst. Technol.*, vol. 29, no. 4, pp. 1549–1564, Jul. 2021.
[40] D. Xu, C. Dai, and H. Su, "Alternate periodic event-triggered control for synchronization of multilayer neural networks," *Inf. Sci.*, vol. 596, pp. 169–184, 2022.
[41] P. Chen, D. Zhang, L. Yu, and H. Yan, "Dynamic event-triggered output feedback control for load frequency control in power systems with multiple cyber attacks," *IEEE Trans. Syst., Man, Cybern., Syst.*, vol. 52, no. 10, pp. 6246–6258, Oct. 2022.
[42] J. Zhang, X. Zhao, and J. Huang, "Synchronization control of neural networks with state-dependent coefficient matrices," *IEEE Trans. Neural Netw. Learn. Syst.*, vol. 27, no. 11, pp. 2440–2447, Nov. 2016.
[43] F. Ding et al., "Event-triggered control for nonlinear leaf spring hydraulic actuator suspension system with valve predictive management," *Inf. Sci.*, vol. 551, pp. 184–204, 2021.
[44] R. Pan, Y. Tan, D. Du, and S. Fei, "Adaptive event-triggered synchronization control for complex networks with quantization and cyber-attacks," *Neurocomputing*, vol. 382, pp. 249–258, 2020.

Yan Li received the Ph.D. degree in computer science from both the University of Science and Technology of China, Hefei, China, and the City University of Hong Kong, Hong Kong, in 2011.

She is currently an Associate Professor with the College of Information Engineering, Nanjing University of Finance and Economics, Nanjing, China. Her research interests include networked control systems, learning-based algorithms, and software-defined networking.

Feiyu Song received the B.S. degree in information management and information system from Nanjing University of Finance and Economics, Nanjing, China, in 2020, where she is currently pursuing the M.Sc. degree in computer science.

Her research interests include complex networks and networked control systems.

Jinliang Liu received the Ph.D. degree in automatic control from Donghua University, Shanghai, China, in 2011.

From 2013 to 2016, he was a Postdoctoral Research Associate with the School of Automation, Southeast University, Nanjing, China. He is currently a Professor with the College of Information Engineering, Nanjing University of Finance and Economics. His research interests include networked control systems, complex dynamical networks, and time-delay systems.

Xiangpeng Xie received the B.S. and Ph.D. degrees in engineering from Northeastern University, Shenyang, China, in 2004 and 2010, respectively.

He is currently a Professor with the Institute of Advanced Technology, Nanjing University of Posts and Telecommunications, Nanjing, China. His research interests include fuzzy modeling and control synthesis, state estimations, optimization in process industries, and intelligent optimization algorithms.

Dr. Xie is an Associate Editor for the *International Journal of Fuzzy Systems* and *International Journal of Control, Automation, and Systems*.

Engang Tian received the B.S. degree in mathematics from Shandong Normal University, Jinan, China, in 2002, the M.Sc. degree in operations research and cybernetics from Nanjing Normal University, Nanjing, China, in 2005, and the Ph.D. degree in control theory and control engineering from Donghua University, Shanghai, China, in 2008.

He is currently a Professor with the School of Optical-Electrical and Computer Engineering, University of Shanghai for Science and Technology, Shanghai. His research interests include networked control systems, cyberattacks, and nonlinear stochastic control and filtering.